Journal of Applied Polymer Science

Effects of Small Molecular Weight Silicon-Containing Acrylate on Kinetics, Morphologies, and Properties of Free-Radical/Cationic Hybrid UV-Cured Coatings

Yuanchun Qi, Lingling Li, Zhou Fang, Jianfeng Zhong, Qingzhi Dong

Shanghai Key Laboratory of Advanced Polymeric Materials, Key Laboratory for Ultrafine Materials of Ministry of Education, School of Materials Science and Engineering, East China University of Science and Technology, Shanghai 200237, People's Republic of China

Correspondence to: Q. Z. Dong (E-mail: qzhdong@ecust.edu.cn)

ABSTRACT: A series of UV-curable, silicon-containing mixtures were prepared by adding different micro amounts of small molecular weight silicon-containing acrylate KH570 to an interpenetrating polymer network system composed of cycloaliphatic polyurethane acrylate, trimethylolpropane triacrylate, cycloaliphatic epoxy resin, free-radical photoinitiator Irgacure 754 and cationic photoinitiator Irgacure 250 with a weight ratio of 15 : 15 : 65 : 1 : 4. Hybrid coatings with different addition amounts of KH570 (0.2, 0.6, 1.0 wt %) were cured from the mixtures by UV-initiated free-radical/cationic dual curing technique. Final reactant conversions and photopolymerization rates of the hybrid UV-cured coatings were improved with the increase of KH570 content, as evaluated by conversion profiles. The morphologies and microstructures were characterized by scanning electron micro-scopic, atomic force micrographic, and fourier transform infrared spectrophotometer measurements. Thermal, mechanical, and surface properties of the hybrid UV-cured coatings were investigated. The increase in KH570 content caused a decrease in mechanical properties besides the breaking elongation. Thermo-gravimetric analysis revealed that the incorporation of silicon into cross-linked network structure resulted in high thermal stability. The surface properties of hybrid UV-cured coatings, such as hardness, contact angle, flexibility, and glossiness were also examined. It is found that transparent hybrid coating with the addition of 1.0 wt % KH570 exhibited a relatively higher contact angle as a direct result of a relatively higher hydrophobic surface. These researches showed that micro amounts of small molecular weight silicon-containing acrylate could greatly influence the morphologies of liquid nitrogen quenching cross sections and properties of hybrid UV-cured coatings and could be used to modify UV-cured coatings for some superior properties. © 2014 Wiley Periodicals, Inc. J. Appl. Polym. Sci. **2014**, *131*, 40655.

KEYWORDS: coatings; crosslinking; kinetics; morphology; photopolymerization

Received 2 October 2013; accepted 27 February 2014
DOI: 10.1002/app.40655

INTRODUCTION

Hybrid polymers have been recognized as an important class of high-performance materials in material chemistry. Most hybrid materials proposed in literatures are thermally cured. Alternatively, hybrid materials prepared by ultraviolet (UV) curing technique are more attractive because of their advantages of instant curing, high efficiency, environmental friendly, flexible formulation, and adjustable performance.[1] These advantages bring about a rapid growth of UV-curing technology in various fields, especially in synthesizing protective coatings for diverse substrates, such as paper, fiber, metal, wood, and plastic.

Nearly all of the reports on UV-cured coatings adopted a separate free-radical or cationic photopolymerization method. Nevertheless, the combination of free-radical and cationic UV curing techniques may achieve preparation of hybrid polymers with unordinary structures, for instance, block copolymer[2], and graft copolymer.[3] Particularly, interpenetrating polymer network (IPN) which is regarded as the most promising material in coating field can also be obtained when the formulation is adjusted to an appropriate composing proportion.[4–7]

UV-initiated free-radical/cationic hybrid curing technique is proceeded by cross-linking polymerization of oligomers or monomers via two distinct mechanisms: free-radical and cationic types. In the first case, acrylates, polyurethane acrylates, polyester acrylates, and acrylic acrylates are commonly used because of their high reactivity, together with the advantage of solvent-free process carried out at room temperature. However, free-radical photopolymerization has an inherent shortcoming

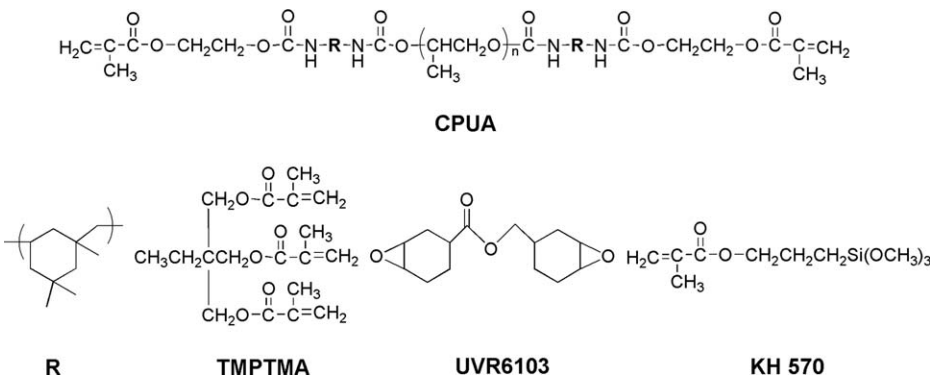

Figure 1. Chemical structures of rude materials.

of cure-induced volume shrinkage. From the view of molecular structure, it could be attributed to the fact that the distance between oligomers or monomers changes from the van der Waals force distance to covalent bond distance during photopolymerization process and in consequence the volume of final product shrinks significantly. Fortunately, cationic UV curing is a good way of remedy to the aforementioned defect. The cationic ring-opening polymerization of epoxide resins reduces volume shrinkage and produces plenty of hydrogen bonds that will increase the adhesion between coatings and substrates. Therefore, UV-initiated free-radical/cationic hybrid curing technique has been gradually taken as the most feasible candidate for large scaled applications.[8]

For producing high integrated performance UV-cured coating, introduction of silicon-containing oligomers or monomers to matrix systems is another very useful method. Silicon-containing materials have peculiar characteristics such as thermal stability,[9,10] weathering resistance,[11,12] flexibility[13], and water impermeability,[14] and they have been used in various applications including high-performance elastomers, membranes, adhesives, antifoams, electrical insulators, water repellants, fire retardants, textile softeners, medical materials and coupling agents.[15–17] There are three types of usual strategies to incorporate silicon into hybrid UV-cured systems in previous studies: (1) mixing silicon dioxide (SiO_2)/polysiloxane with some photopolymerization oligomer to form inorganic–organic hybrid systems[9,18]; (2) preparing silicon-containing acrylates by Michael-type addition reaction between polysiloxane and acrylate for free-radical photopolymerization[19–21]; and (3) preparing silicon-containing epoxide or vinyl ether by hydrosilation reaction between polysiloxane and epoxide/vinyl ether for cationic photopolymerization.[13,22–24] However, most of these techniques are not suited to practical application because the step-by-step syntheses of silicon-containing oligomers restrict industrial production on a large scale.

According to what we have learnt, there is little literature available regarding low molecular weight silicon-containing acrylate just as an additive. In our thesis, different micro amounts of low molecular weight silicon-containing acrylate KH570 were directly added to a UV-curable mixture of cycloaliphatic polyurethane acrylate (CPUA), trimethylolpropane triacrylate (TMPTMA), cycloaliphatic epoxy resin (CER), free-radical photoinitiator Irgacure 754 and cationic photoinitiator Irgacure 250 with a weight ratio of 15 : 15 : 65 : 1 : 4. It has optimum comprehensive properties in the series of CPUA/TMPTMA/CER hybrid coatings with different component ratios. Transparent hybrid coatings were prepared by the UV-initiated free-radical/cationic dual curing technique. The blend of oligomer CPUA and reactive diluent TMPTMA at a weight ratio of 1 : 1, polymerized by a free-radical mechanism, whereas CER UVR6103 polymerized by a cationic mechanism. Silicon-containing acrylate KH570, generally used as silane coupling agent in aqueous solution,[10,25] here was added in the nonsolvent system and copolymerized with CPUA or TMTPTMA. It was found that the increase in silicon-containing acrylate content caused a decrease of the cross-linking densities in the UV-cured coatings, which leads to a decrease in the storage modulus and the tensile strength. Pendant group of

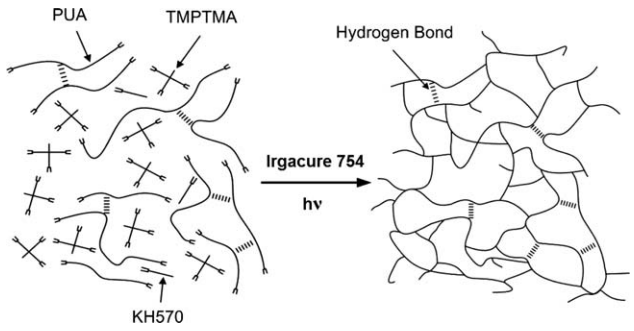

Scheme 1. Silicon-containing UTC polymer network formed by free-radical photopolymerization of the mixture of CPUA, TMPTMA, and KH570.

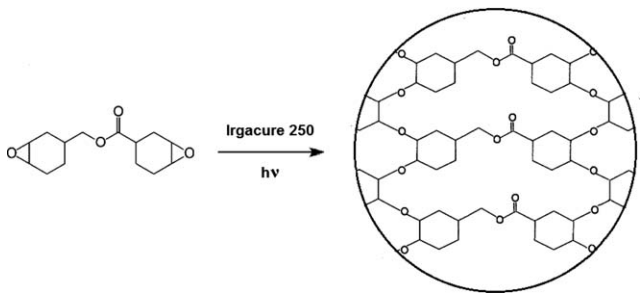

Scheme 2. CER polymer network formed by cationic photopolymerization of UVR6103.

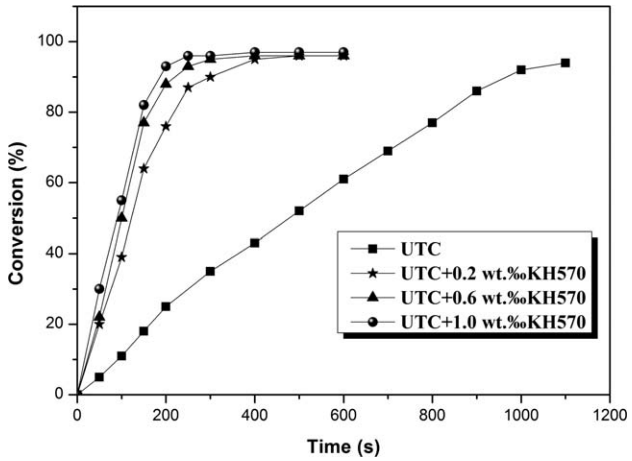

Figure 2. Influence of additive weight ratio of KH570 on conversions of the hybrid UV-cured coatings.

KH570 molecule in the network not only decreases the density of cross-links but also acts as plasticizers, causing greater extensions prior to break.[14] So the silicon-containing hybrid UV-cured coatings above mentioned became softer and even may be cracked when the additive amount of KH570 is more than 1.0 wt %. The objective of this research is to study the influence of micro amount of additive KH570 to morphologies and properties of the hybrid UV-cured coatings. Photopolymerization kinetics, surface morphologies and liquid nitrogen quenching cross section morphologies were carefully analyzed. At the same time, the mechanical, thermal and surface properties of the hybrid UV-cured coatings obtained via the UV-initiated free-radical/cationic dual curing technique were investigated.

EXPERIMENTAL

Materials

Isophorone diisocyanate (IPDI) and polypropylene glycol 1000 (PPG1000) were dried and degassed at 80°C for 2 h; 2-hydroxyethyl methacrylate (HEMA) was used to introduce double bond into oligomer; TMPTMA was used as reactive diluent and purchased from Shanghai Jiachen Chemical Industry, China. 4-Epoxycyclohexylmethyl-3, 4-epoxycyclohexanecarboxylate (UVR6103) was purchased from Hubei Xinjing Advance Materials, China. Dibutyltin dilaurate (DBTDL) and methyl ether hydroquinone (MEHQ) were purchased from Sinopharm Chemical Regent, China. Irgacure 754 (a mixture of oxy-phenyl-acid 2-[2oxo-2phenyl-acetoxy-ethoxyl]-ethyl ester and oxy-phenyl-acetic 2-[2hydroxy-ethoxy]-ethyl ester, Ciba, USA) was used as free-radical photoinitiator and Irgacure 250 (iodonium salt, Ciba, USA) was used as cationic photoinitiator. 3-methacryloxypropyl trimethoxy silane (KH570) was obtained commercially and used without further treatment.

Preparation of CPUA

About 22.30 g IPDI (0.10 mol), 50.00 g PPG1000 (0.05 mol), and a drop of DBTDL were set in a 250 mL glass round flask with four outlets and stirred for half an hour, and then the reaction temperature was increased up to 80°C under nitrogen atmosphere and maintained until NCO value reached theoretic value. Next, the above mixture was cooled to 50°C, and 13.00 g HEMA (0.1 mol), 0.02 g MEHQ and a drop of DBTDL were added. The reaction was kept at this temperature until NCO vanished. The chemical structure of CPUA was shown in Figure 1.

Preparation of the Hybrid UV-Cured Coatings

The CPUA/TMPTMA/CER hybrid coating, coded as UTC, was formed from the mixture of CPUA (15 wt %), TMPTMA(15 wt %), UVR6103 (65 wt %), free-radical photoinitiator Irgacure 754 (1 wt %), and cationic photoinitiator Irgacure 250 (4 wt %). The chemical structures of TMPTMA, UVR6103, and KH570 were also shown in Figure 1. A series of hybrid UV-cured coatings were prepared by adding different micro amounts of the silicon-containing acrylate KH570 (0.2, 0.6, 1.0 wt %) to the UTC hybrid coating. The crude materials were poured into Teflon mold to form cuboids for testing thermal and mechanical properties; meanwhile, the crude materials are leveled into even layers on tinplate sheet for testing surface properties. And then all the samples were cured under a high pressure mercury lamp emitting light at 365 nm. The thickness of these fully cured hybrid coatings measured by micrometer were all about 30 μm. The formation processes of the UTC polymer network and CER polymer network were given in Scheme 1 and Scheme 2, respectively.

Analysis

The conversion of C=C and epoxy were calculated by taking the ratio of the functional group absorbance at a given time (A_t) to the initial absorbance (A_0), and the conversions of hybrid UV-cured coatings were calculated based on the conversion of C=C and epoxy groups[26,27]:

$$\chi_{C=C(t)} = \left(1 - \frac{A_t^{1635}}{A_0^{1635}}\right) \times 100 \quad (1)$$

$$\chi_{epoxy(t)} = \left(1 - \frac{A_t^{798}}{A_0^{798}}\right) \times 100 \quad (2)$$

$$\text{Conversion } (\%) = \chi_{C=C(t)} \cdot n_{C=C}\,(\text{mol}\,\%) + \chi_{epoxy\,(t)} \cdot n_{epoxy}\,(\text{mol}\,\%) \quad (3)$$

where $\chi_{(t)}$ is the conversion of these reactive functions at t time, A_0 is the initial absorbance (before UV irradiation), and A_t is

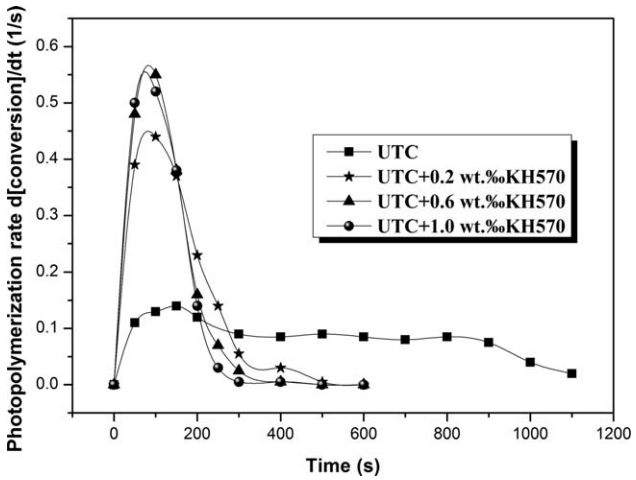

Figure 3. Influence of additive weight ratio of KH570 on photopolymerization rates of the hybrid UV-cured coatings.

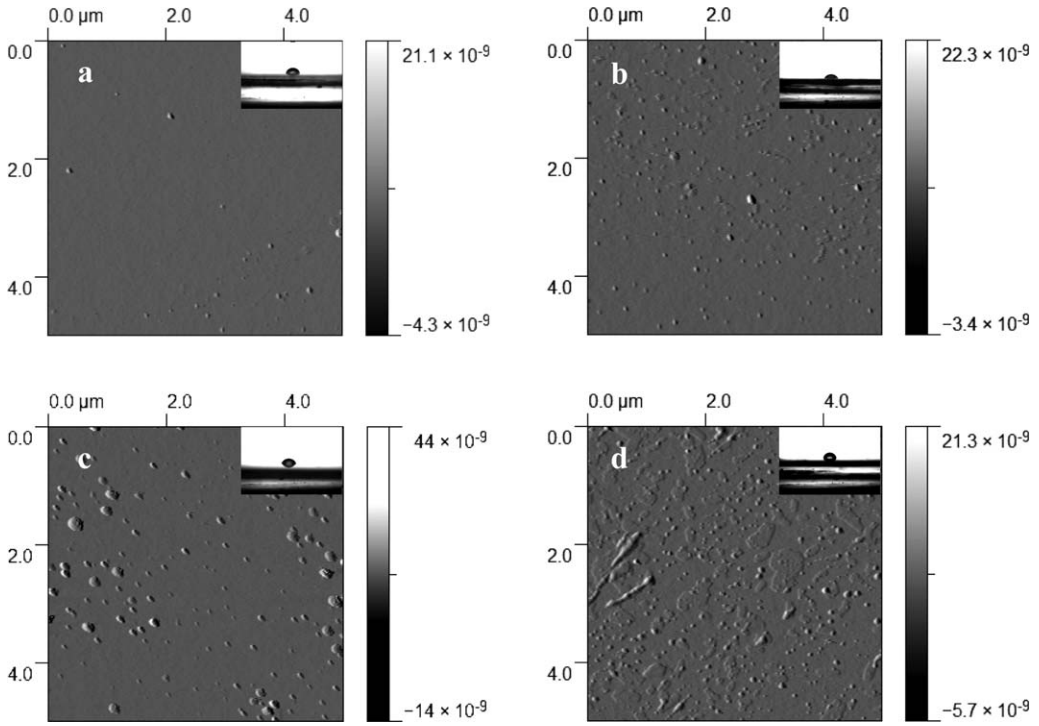

Figure 4. The AFM images of the hybrid UV-cured coatings: (a) UTC, (b) UTC+0.2 wt % KH570, (c) UTC+0.6 wt % KH570, and (d) UTC+1.0 wt % KH570.

the absorbance of the functional group at t time, n is the mole fraction of C=C and epoxy functional groups in different hybrid UV-cured systems.

Atomic force micrography (AFM) measurements of surface morphologies of the hybrid UV-cured coatings were examined by using a Digital Instruments NanoScope IIIa scanning probe microscope.

Scanning electron micro-scope (SEM) observations of cross section morphologies were carried out using Anova NanoSEM 450 scanning electron microscope (FEI Company, America). Bulk UV-cured materials were plunged into liquid nitrogen and their quenching cross sections were investigated.

Fourier transform infrared spectrophotometer (FT-IR) spectra of the hybrid UV-cured coatings were recorded using a Nicolet 5700 spectrometer (America) between 4000 and 650 cm^{-1} with a total of 64 scans at a resolution of 1 cm^{-1} in the transmission mode.

Thermogravimetric analysis (TGA) data of the hybrid UV-cured coatings were performed with a Mettler-Toledo TGA/SDTA 851 instrument (Switzerland) from ambient temperature to 600°C at a heating rate of 10°C /min under normal nitrogen atmosphere according to ASTM E2402-2005.

The stress–strain data were measured by CSS-44100 electronic universal test machine which was made by Changchun Research Institute of Testing Machines (China) according to ASTM D638-2003.

Dynamic mechanical analysis (DMA) curves were performed on a DMA2980 analyser of TA (America) over a temperature range from −80°C to 200°C with a heating rate of 3°C/min at 1 Hz according to ASTM D5418-2007. The UV-curable mixtures were cured as rectangular bars (6.0 cm × 1.0 cm ×0.3 cm).

Pencil hardness data of the hybrid UV-cured coatings were evaluated by QHQ-A pencil hardness tester which made by Tianjin Yonglida Material Testing Machine (China) according to ASTM D3363-2005.

Pendulum hardness data of the hybrid UV-cured coatings were investigated by pendulum hardness tester BYK 5858 (Germany) according to ASTM D4366-1995.

Flexibility data of the hybrid UV-cured coatings were conducted on a QTY-10A cylindrical bending test device which was made by Shanghai Instrument (China) according to ASTM D4145-2010.

Contact angle data of the hybrid UV-cured coatings were measured by Rame-hart model 100 contact angle goniometer (America) according to ASTM D5725-1999.

The glossiness data of the hybrid UV-cured coatings were tested by digital glossiness meter 4430 (Germany) according to ASTM D2457-2003.

RESULTS AND DISCUSSION

Photopolymerization Kinetics

Figures 2 and 3 show UV curing kinetics of the silicon-containing hybrid coatings with different concentrations of KH570. It is obvious that the addition of KH570 has positive influence on reactant conversions and polymerization rates of the hybrid UV-cured coating systems, which increased

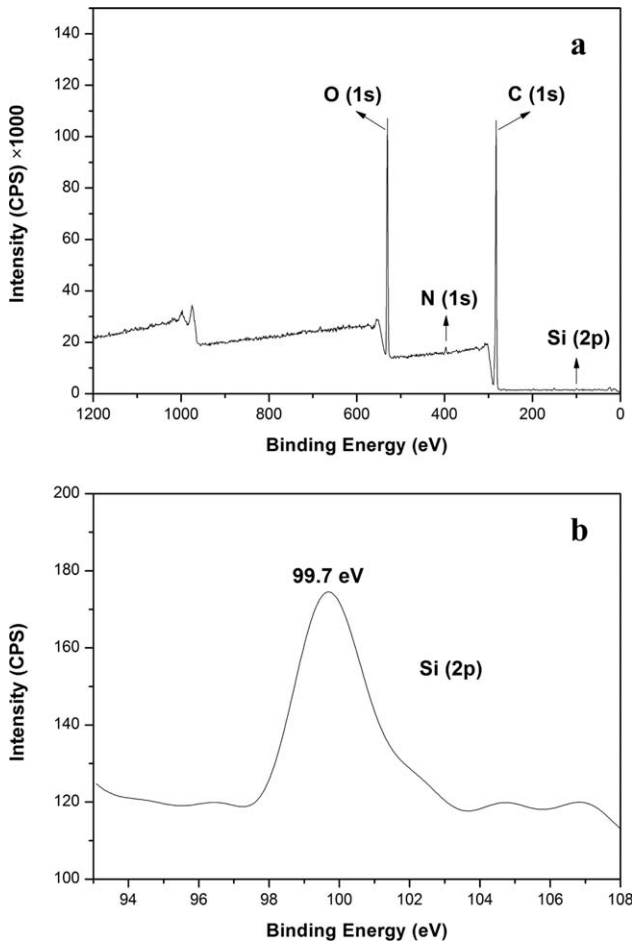

Figure 5. Representative (a) XPS wide-scan spectrum of the silicon-containing hybrid UV-cured coatings and the corresponding (b) high-resolution XPS spectrum of Si (2p) peak.

significantly with the increasing KH570 content. This increase could be explained by the steric inhabitation effect of trimethoxy silane pendant group in KH570 molecule, leading to flexible network structure and high mobility of reactive species. In photopolymerization process of UTC hybrid UV-curable system, at first oligomers and monomers are incorporated into polymer chains as units containing pendant bonds, then they are formed into networks with large polymer chains entangled and cross-linked in short time. The mobility of free radical and cationic photoinitiators, unreacted oligomers and monomers are hindered by the cross-linked networks to a certain extend.[28] However, the existence of relatively larger volume of trimethoxy silane pendant group of KH570 interrupts intermolecular hydrogen bonds consisting of a hydrogen atom between electronegative atoms in CPUA, TMPTMA, CER, and KH570, decreases the cross-linking density of cross-linked networks and provides enough space for photoinitiators and unreaced oligomers and monomers entering and leaving networks. Therefore, the conversion versus time graph of UTC hybrid UV-curable system is similar linear, while the silicon-containing hybrid UV-curable systems have auto-acceleration phenomena and their photopolymerization rates reach their maximum between 20% and 50% conversion, as can be seen in conversion change curves and photopolymerization rate curves. In conclusion, the concentration of KH570 plays an important role in the photopolymerization kinetics because it accelerates the rate of chain extension and termination, leading to rapid cross-linking processes.

Surface Morphologies

The surface morphologies of the hybrid UV-cured coatings were evaluated by means of AFM, as shown in Figure 4. AFM micrographs indicated that there were few particles jutting from the smooth surface of UTC hybrid coating, which may be because of the existence of photoinitiators, whereas on the surface of the silicon-containing hybrid coatings a large number of polysiloxane particles, photopolymerized from the additive KH570, were homogeneously dispersed on the surface of UTC matrix. For the surface morphology of 0.2 wt % KH570-containing hybrid coating, the polysiloxane particles with an average diameter of 120 nm in the range of 80–200 nm were observed. When the adding amount increased to 0.6 wt %, the polysiloxane particle size increased to a larger average diameter of 200 nm in the range of 80–300 nm. Furthermore, for 1.0 wt % KH570-containing hybrid coating, polysiloxane particles were enlarged and aggregated into blocks. Evidently, micro amounts of KH570 can bring about great changes to the surface morphologies of hybrid UV-cured coatings and the corresponding surface performances. With further analysis, the difference between bulk concentration and surface concentration of KH570 is probably because the most KH570 molecules migrate to the coating surface during photopolymerization process for its low surface energy.[29,30]

As shown in Figure 5, the representative XPS wide-scan spectrum of the hybrid UV-cured coatings (a) shows the presence of the Si (2p) peak, and the corresponding high-resolution XPS spectrum (b) presents the Si (2p) peak at 99.5 eV, which is attributed to Si-C bonding.[31] Theoretical atomic ratios for the three silicon-containing hybrid systems UTC+0.2 wt % KH570, UTC+0.6 wt % KH570, and UTC+1.0 wt % KH570 prior to conversion, calculated from the stoichiometry, were 0.0015, 0.0048, and 0.0063 at %, respectively. The percentages of Si (2p) measured by XPS were 0.22, 1.05, and 3.21 at %, which are extremely high in comparison with the value obtained from stoichiometry. This result coincides with the surface morphologies of silicon-containing hybrid UV-cured coatings and proves that KH570 molecules would migrate from interior to coating surfaces with cross-link proceeding.

Liquid Nitrogen Quenching Cross-Section Morphologies

SEM measurement is helpful for the internal structure analyses of hybrid UV-cured coatings. As shown in Figure 6, the neat UTC hybrid coating derived from free-radical/cationic hybrid photopolymerization presented a relatively flat and compact liquid nitrogen quenching cross section with visibly IPN microstructure. Nevertheless, with the incorporation of KH570 to the formulation of UTC hybrid coating, the liquid nitrogen quenching cross section changed from a smooth one to rough surfaces accompanying with a large quantity of cavities and gaps. The copolymerization of KH570 and crude materials containing double bonds, introduces siloxane lateral group with easily rotary silicon-oxygen bond and free volume cavities into the

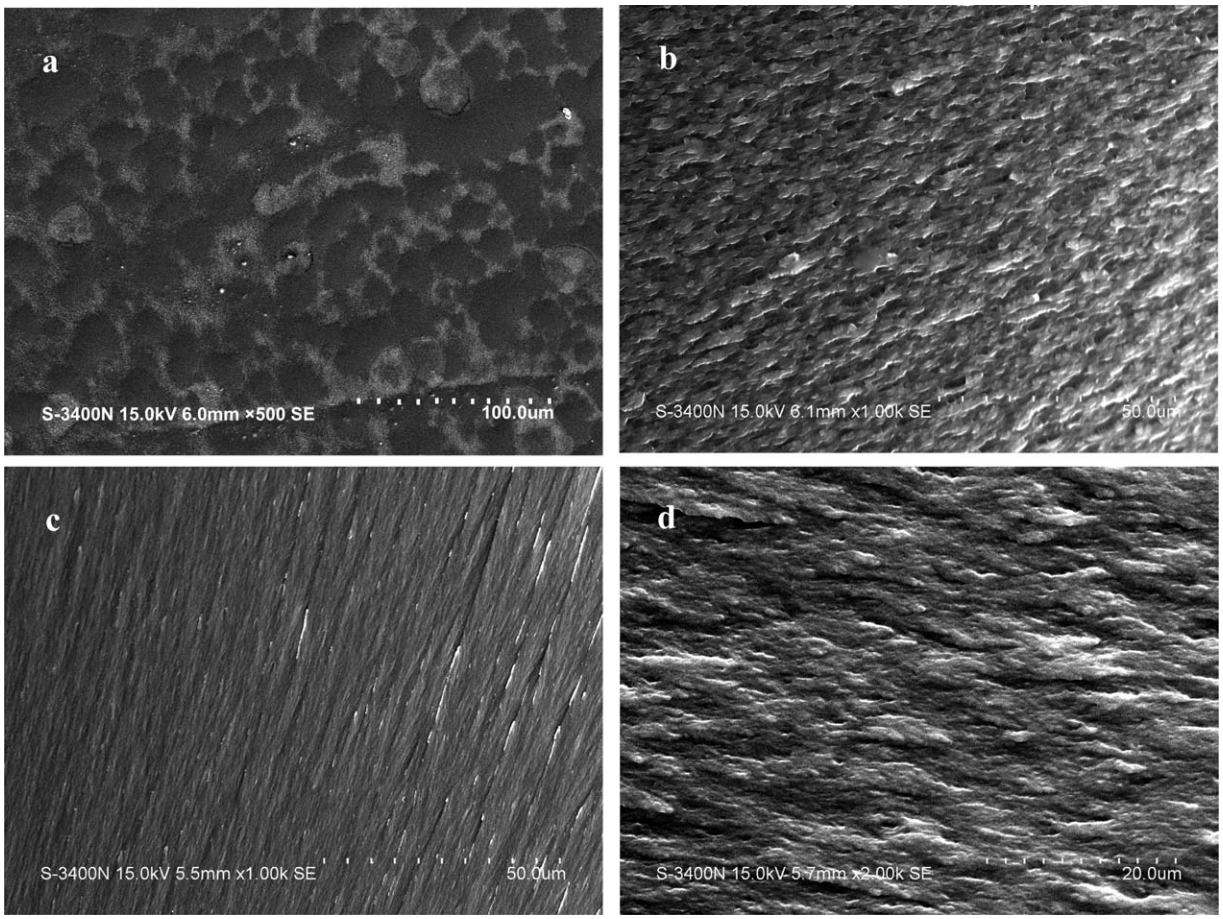

Figure 6. The SEM pictures of cross sections of the hybrid UV-cured coatings: (a) UTC, (b) UTC+0.2 wt %KH570, (c) UTC+0.6 wt % KH570, and (d) UTC+1.0 wt % KH570.

IPN network of UTC hybrid coating, and thus makes the hybrid system absorb more energy under external force.[14] The unconformity between liquid nitrogen quenching cross section morphologies and surface morphologies confirms the speculation that the KH570 molecules migrate from the interior to the surface of UTC hybrid coating during photopolymerization process.

For further investigation, with the increasing KH570 content, the liquid nitrogen quenching cross sections of silicon-containing hybrid coatings tended to be smooth and compact. The trimethoxylsilane pendant group in KH570 molecule brings two contrary influences on the microstructure of the cross-linked network, steric hindrance effect and hydrogen bond interaction.[32] The hydrogen bonds between -COO- in KH570, -NH-, -COO-, -C-O-C- in CPUA/TMPTMA and -C-O-C-, -OH in CER, are hindered by the steric hindrance effect of siloxane lateral group in KH570. With the increase of KH570 content, hydrogen bond interaction generally becomes a dominate factor. In a word, both of the two factors are related with the concentration of KH570, hence the microstructures of hybrid UV-cured coatings are closely dependent on the KH570 contents.

FT-IR Spectra

The FT-IR spectra in the range of 4000–500 cm^{-1} of the hybrid UV-cured coatings are shown in Figure 7. The representative peak, the bending frequency of Si-O-CH_3 group at 965 cm^{-1}, was not observed.[25] The stretching vibration peak of Si-O-CH_3 at 1083 cm^{-1} also did not appear, which may be covered by the characteristic peak of epoxy group at 1086 cm^{-1}.[6,9] Meanwhile,

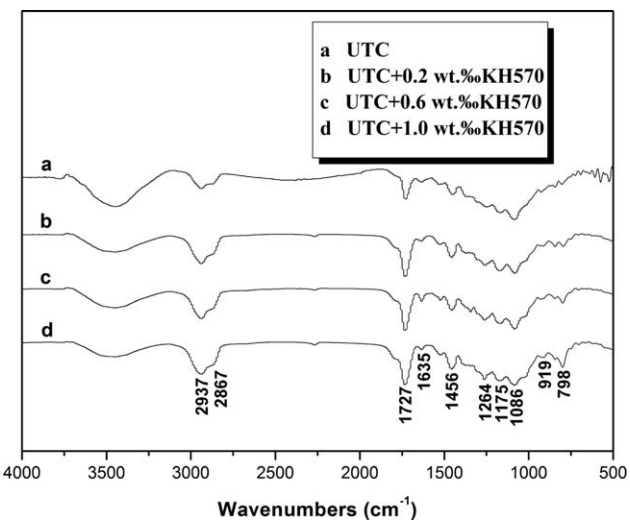

Figure 7. FT-IR spectra of the hybrid UV-cured coatings: (a) UTC, (b) UTC+0.2 wt % KH570, (c) UTC+0.6 wt % KH570, and (d) UTC+1.0 wt % KH570.

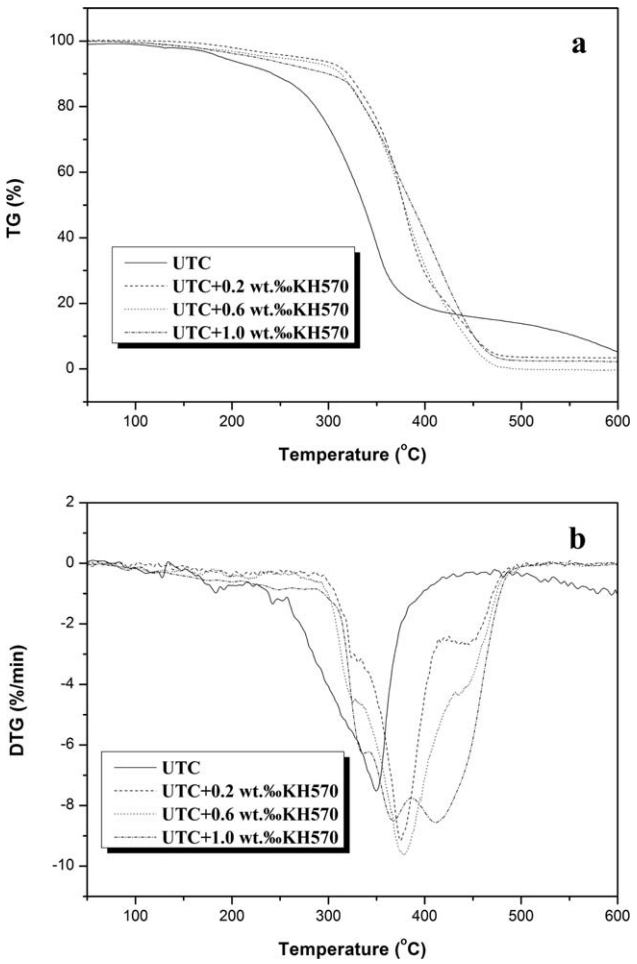

Figure 8. (a) TG and (b) DTG curves of the hybrid UV-cured coatings under nitrogen flow.

the characteristic vibration peak of Si-CH_2 at 798 cm^{-1} gradually became sharp with the increasing KH570 content. Above phenomena demonstrate that KH570 molecules have been introduced into the free-radical copolymerized network of UTC hybrid coating. The intensity of the absorbance for C=C vibration at 1635 cm^{-1} decreased with the increase of KH570 content, implying relatively complete free-radical copolymerization of KH570 with CPUA/TMPTMA blend under UV radiation. These are in accordance with the conclusion of kinetic investigation.

In addition, the characteristic bands in 2937–2867 cm^{-1} were attributed to asymmetrical and symmetrical stretching vibration of the aliphatic CH_2 and CH_3 groups,[33] while the peak 1727 cm^{-1} was attributed to C=O stretching vibration in CER. Asymmetrical and symmetrical C-H stretching vibration of C-O-C bonds were observed at 1264 and 1086 cm^{-1} because of the high C-O-C content originating from cationic open-ring polymerization. The peaks at 1456 and 1175 cm^{-1} were ascribed to scissor bending vibration and bending vibration of CH_2, respectively.[6]

Thermal Behaviors

TGA is commonly used as an important technique to evaluate thermal stability of diverse materials. Figure 8 shows the TG (a) and DTG (b) thermograms of hybrid UV-cured coatings with various KH570 contents and corresponding data are collected in Table I. As seen from Table I, all the silicon-containing hybrid coatings presented a small weight loss below 300°C, indicating their almost complete conversion with few volatile degradation products such as unreacted oligomer, reactive diluent, and photoinitiators. The temperatures which corresponded to 5%, 50%, and 90% weight loss for silicon-containing hybrid coatings were observed in ranges of 210–280°C, 370–390°C, and 440–460°C, respectively. Under the same atmosphere, the temperatures of 5%, 50%, and 90% weight loss for neat UTC hybrid coating were discovered at 190°C, 336°C, and 350°C, respectively. The main initial degradation step for the silicon-containing hybrid coatings was observed in the range of 300–320°C which is much higher than the initial temperature for UTC hybrid coating. In previous studies,[9,13] it is generally thought that the silicon-containing compounds in the UV-curable system improved the thermal stability of matrix material, which is attributed to the insertion of siloxane moieties in the UV-cured network, as well as to the silica formation during thermal degradation that induced an oxidation process retardation and an insulation effect. Similarly, in our system the delay of thermal degradation should be also assigned to the introduction of small molecular weight additive silicone-containing acrylate KH570 as aforementioned explanation. It is obvious that micro adding amount of KH570 hardly has any influence on residue weight of the hybrid UV-cured coatings, so microstructure is the major determinant to influence the residue weights of hybrid UV-cured coatings. Furthermore, SEM photos expressed that the cross-linking density of network structures is decreased because of the steric hindrance effect of trimethoxy silane pendant group. As a consequence, the residue weights of the silicone-containing hybrid coatings decreased evidently in the range of 300–500°C and stabled at a constant low value above 500°C. Although the lower cross-linking density of silicon-containing

Table I. The TGA Results of the Hybrid UV-Cured Coatings

Coatings	$T_{5\%}$ (°C)	$T_{50\%}$ (°C)	$T_{90\%}$ (°C)	T_{in} (°C)	T_{max} (%)	Residue (%), 600°C
UTC	190	336	556	173	350	5.3
UTC+0.2 wt %KH570	272	377	451	308	374	3.3
UTC+0.6 wt %KH570	246	378	442	300	379	0.1
UTC+1.0 wt %KH570	225	387	451	313	368,413	2.4

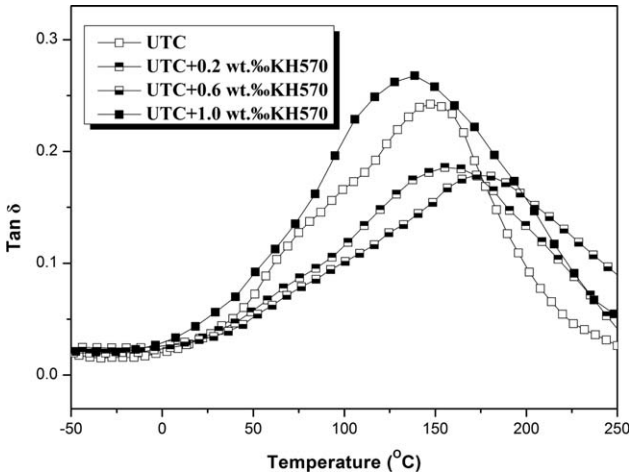

Figure 9. DMA curves of the loss factor tan δ for hybrid UV-cured coatings.

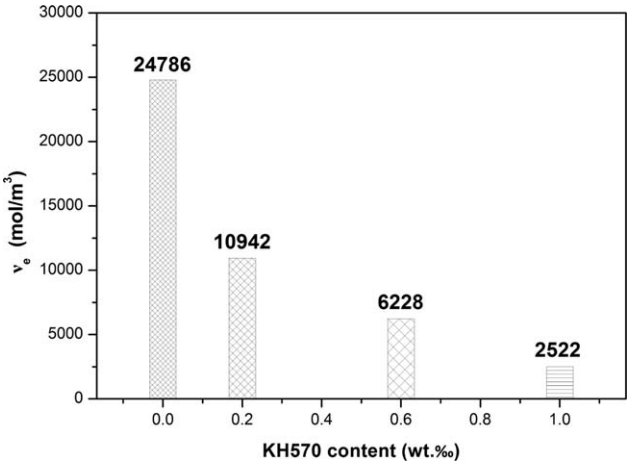

Figure 11. Influence of additive weight ratio of KH570 on cross-linking densities of the hybrid UV-cured coatings.

hybrid coatings bring less residue, but the influence to thermal stability is much little than insulation effect of silica.

Mechanical Properties

T_g value is taken as the peak temperature in the plots of tan δ versus temperature obtained from DMA test. In Figure 9, there was only one damping peak for all hybrid UV-cured coatings, implying good miscibility among the blend of CPUA/TMPTMA, the monomer CER and the additive KH570. Each damping peak of the hybrid UV-cured coatings was asymmetric and could be divided into multiple peaks, illuminating that no component in these systems occupies the dominant percent. UTC hybrid coating shows a relatively narrow damping peak with a large intensity at 148°C with an additional shoulder at the side of low temperature, which corresponds to the interior morphology of contact IPN structure as shown in Figure 3(a). The incorporation of KH570 damaged the bi-continuous network and exhibited complex microstructures with cavities and gaps, causing broad and asymmetrical tan δ peaks. The damping peaks of silicon-containing hybrid coatings with the addition of 0.2 and 0.6 wt % KH570 were detected at temperature 155°C and 171°C with relatively lower intensities, which are higher than UTC hybrid coating at 148°C. The steric hindrance effect of siloxane lateral group improves the segment mobility of the network, leading to relatively higher T_g value and lower intensity tan δ peak. This means that the intensity of damping peak reflects the difficulty in segment mobility. The higher the intensity of damping peak, the bigger the difficulty of segment mobility will be.[34] Whereas, when KH570 content was increased to 1.0 wt %, T_g was shift to 136°C and the intensity of corresponding damping peak was stronger than UTC hybrid coating. This could be attributed to the coalescent of KH570 molecules which provides enough hydrogen bond interactions to counterbalance steric hindrance effect of siloxane lateral group and improves segment mobility of polymer molecular chains.

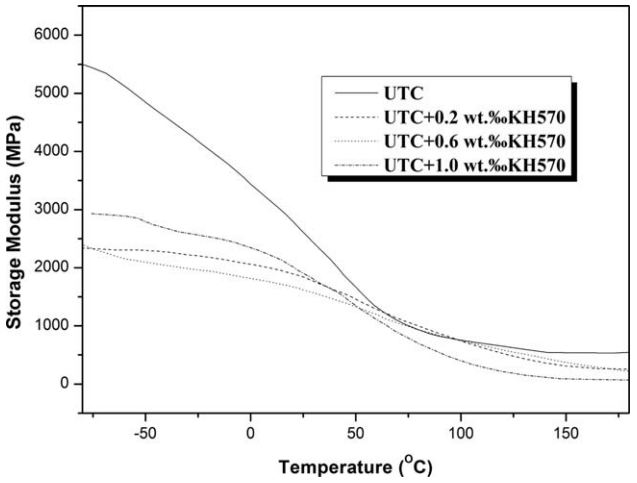

Figure 10. DMA curves of the loss factor storage modulus E' for hybrid UV-cured coatings.

It is well acknowledged that the storage modulus of a polymer in the glassy state reflects its stiffness. A high storage modulus (relative rigidity) means a high microphase separation degree.[35] Figure 10 shows the variance of modulus with temperature for the hybrid UV-cured coatings. The decrease of double bond content and cross-linking density in silicon-containing hybrid coatings is caused by the incorporation of KH570 which has only one double bond per molecule, resulting in a decrease in the storage modulus. Remarkably, although only minimum KH570 was introduced into the hybrid UV-cured coatings, it has exerted tremendous influence on the microstructures and properties.

According to cross-linked network theory, with the cross-linking density increases, the coupling between the rubber molecule chains become denser and form three-dimensional network structure, limiting the movement of the molecular chains. Therefore, the resulting deformation modulus can be improved under certain stress. The cross-linking density, v_e, was calculated from the measured storage modulus E' under the temperature T (T_g+40°C), through an equation derived from the theory of rubber elasticity[36]:

$$v_e = E'/6RT \quad (4)$$

where R is the gas constant, 8.314 J·mol^{-1}·K^{-1}; T is the temperature that 40°C higher than glass transition temperature,

Table II. Mechanical Properties of the Hybrid UV-Cured Coatings

Coatings	Tensile strength (MPa)	Breaking elongation (%)	Storage modulus E' (MPa)	T_g (DMA) (°C)
UTC	24.00	3.59	5501	148
UTC+0.2 wt % KH570	22.55	4.27	2328	155
UTC+0.6 wt % KH570	22.17	5.11	2379	171
UTC+1.0 wt % KH570	20.33	6.48	2943	136

Table III. Surface Properties of the Hybrid UV-Cured Coatings

Coatings	Pencil hardness	Pendulum hardness (s)	Flexibility	Glossiness
UTC	5H	152	6	106
UTC+0.2 wt % KH570	5H	152	7	102
UTC+0.6 wt % KH570	5H	147	7	101
UTC+1.0 wt % KH570	5H	135	7	98

measured in K. The effects of chain ends, main-chain scission, and trapped chain entanglements acting as cross-links are omitted, thus giving a quantitative error in the determinations of pure cross-linking concentration.[37] As can be seen in Figure 11, the hybrid UV-cured coatings all had high cross-linking densities and the cross-linking densities decreased with the silicon-containing acrylate KH570 content increasing. The result supports the conclusion from SEM analysis.

The tensile properties were also affected by silicon-containing acrylate composition, as shown in Table II. The ultimate tensile strength of neat UTC hybrid coating was 24.00 MPa, and the breaking elongation value was 3.59%. This result means that the UTC hybrid coating is a kind of hard material with a reasonable degree of flexibility. And the addition of KH570 decreased the cross-linking density of UTC hybrid network, showing lower tensile strength and larger breaking elongation.

Surface Properties

Surface properties of the hybrid UV-cured coatings have been measured as those listed in Table III. The hardness of coatings, which will affect the surface abrasion and scratch resistance, depended on the chain flexibility of molecules, cross-linking density, and hydrogen bonding.[38] It is found that for the hybrid UV-cured coatings micro amount of KH570 has little influence in the pencil hardness, pendulum hardness, which because of the existence of a large number of hydrogen bonds.

The effect of KH570 concentration on the wettability was investigated by contact angle test, and each contact angle value given in Figure 12. The contact angle measured on the air side clearly depends on the surface morphologies of hybrid UV-cured coatings. Contrasting to Figure 3, UTC hybrid coating has a fairly polar surface and shows a water contact angle of $75° \pm 4°$. In the case of silicon-containing hybrid coatings with 0.2 wt % and 0.6 wt % KH570, the contact angle values were $55° \pm 3°$ and $63° \pm 3°$, respectively. The decrease could be explained by the fact that waters filter through hybrid UV-cured coatings and form a large number of hydrogen bonds with electronegative atoms. The contact angle of the hybrid UV-cured coatings containing 1.0 wt % of KH570 increased to $82° \pm 5°$, which higher than expected on the basis of the coating composition. The result illustrates that the cross-linking density, surface morphologies, and liquid nitrogen quenching cross-section morphologies decide wettability of the hybrid UV-cured coatings. However, the silicon-containing molecule KH570 contains only one silicon atom, so it cannot obtain a complete hydrophobic surface.

UTC hybrid coating has good flexibility because of the flexible characteristic of polyether structure in CPUA. Meanwhile, the trimethoxy silane pendant group in additive KH570, attributed to the free and rotation around the silicon oxygen bond, also provides good flexibility to the hybrid UV-cured coatings.

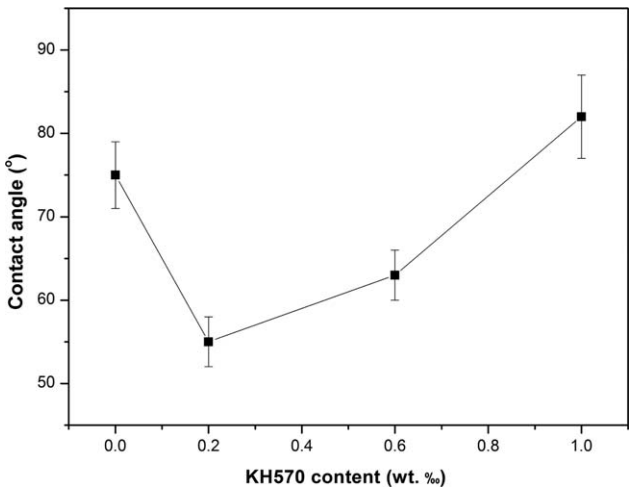

Figure 12. Influence of additive weight ratio of KH570 on water contact angles of the hybrid UV-cured coatings.

Coating's glossiness is a complex phenomenon resulting from the interaction between light and the surface of the coating, affected strongly by surface roughness. The reduction of glossiness with the introduction of KH570, could be assigned to the decrease of cross-linking density and the increase of surface toughness. This trend is consistent with those morphological depictions observed in AFM investigations.

CONCLUSIONS

Micro amounts of silicon-containing acrylate KH570 were used as an additive in a UV-curable system composed of CPUA/TMPTMA/CER. A series of hybrid UV-cured coatings with varied amounts of KH570 were prepared via a UV-initiated free radical/cationic dual curing technique. The addition of silicon-containing acrylate KH570 resulted in excellent UV-curing behaviors, as seen from their fast curing rates and high final conversions. The IPN microstructure of UTC hybrid coating changed definitely with the increasing KH570 content. The surface and liquid nitrogen quenching cross-section morphological studies indicated that the silicon-containing acrylate KH570 migrated to top layers of the hybrid UV-cured coatings during the photopolymerization process. TG and DTG plots of the silicon-containing hybrid UV-cured coatings provided better thermal stability. The decreasing cross-linking density with the increasing weight permillage of KH570 caused a decrease in mechanical properties, excepting for breaking elongation. In conclusion, properties of the silicon-containing hybrid UV-cured coating materials, such as damping capacity and thermal stability were improved, as well as wettability in a specific proportion.

ACKNOWLEDGMENTS

The authors gratefully acknowledge (1) Shanghai Leading Academic Discipline Project (B502); (2) Shanghai Key Laboratory Project (08DZ2230500) China.

REFERENCES

1. Decker, C. *Macromol. Rapid Commun.* **2002**, *23*, 1067.
2. Hawker, C. J.; Hedrick, J. L.; Malmström, E. E.; Trollsås, M.; Mecerreyes, D.; Moineau, G.; Dubois, P.; Jérôme, R. *Macromolecules* **1998**, *31*, 213.
3. Mecerreyes, D.; Pomposo, J. A.; Bengoetxea, M.; Grande, H. *Macromolecules* **2000**, *33*, 5846.
4. Decker, C.; Nguyen Thi Viet, T.; Decker, D.; Weber-Koehl, E. *Polymer* **2001**, *42*, 5531.
5. Zhang, J.; Peppas, N. A. *J. Biomater. Sci. Polym.. Ed.* **2002**, *13*, 511.
6. Duan, J. K.; Kim C.; Jiang, P. K. *J. Polym. Res.* **2009**, *16*, 45.
7. Tehfe, M. A.; Lalevée, J.; Telitel, S.; Contal, E.; Dumur, F.; Gigmes, D.; Bertin, D.; Nechab, M.; Graff, B.; Morlet-Savary, F.; Fouassier, J. P. *Macromolecules* **2012**, *45*, 4454.
8. Guenthner, A. J.; Hess, D. M.; Cash, J. *J. Polymer* **2008**, *49*, 5533.
9. Bayramoğlu, G.; Kahraman, M. V.; Apohan, N. K.; Güngör, A. *Prog. Org. Coat.* **2006**, *57*, 50.
10. Yang, Z. H.; Ni, A. Q.; Wang, J. H. *J. Appl. Polym. Sci.* **2013**, *127*, 2905.
11. Park, H. S.; Kim, S. R.; Park, H. J.; Kwak, Y. C.; Hahm, H. S.; Kim, S. K. *J. Coat. Technol.* **2003**, *75*, 55.
12. Huang, W.; Zhang, Y.; Yu, Y. Z.; Yuan, Y. *J. Appl. Polym. Sci.* **2007**, *104*, 3954.
13. Sangermano, M.; Bongiovanni, R.; Malucelli, G.; Roppolo, I.; Priola, A. *Prog. Org. Coat.* **2006**, *57*, 44.
14. Liu, H. B.; Chen, M. C.; Huang, Z. T.; Xu K.; Zhang, X. *J. Eur. Polym. J.* **2004**, *40*, 609.
15. Hoffmann, F.; Cornelius, M.; Morell, J.; Fröba, M. *Angew. Chem. Int. Ed.* **2006**, *45*, 3216.
16. Asefa, T.; Tao, Z. M. *Can. J. Chem.* **2012**, *90*, 1015.
17. Shit, S. C.; Shah, P. *Natl. Acad. Sci. Lett.* **2013**, *36*, 355.
18. Liu, P.; Gu, A. J.; Liang, G. Z.; Guan, Q. B.; Yuan, L. *Prog. Org. Coat.* **2012**, *74*, 142.
19. Wang, W. Z. *Eur. Polym. J.* **2003**, *39*, 1117.
20. Hong, J. W.; Kim, H. K. *Macromol. Res.* **2006**, *14*, 617.
21. Tang, C. Y.; Liu, W. Q. *J. Coat. Technol. Res.* **2010**, *7*, 651.
22. Connell, J. W.; Crivello, J. V.; Bi, D. *J. Appl. Polym. Sci.* **1995**, *57*, 125.
23. Chiang, C. L.; Ma, C. C. M.; Wang, F. Y.; Kuan, H. C. *Eur. Polym. J.* **2003**, *39*, 825.
24. Braun, H.; Yagci, Y. S.; Nuyken, O. *Eur. Polym. J.* **2002**, *38*, 151.
25. Wan, T.; Lin, J. H.; Li, X. J.; Xiao, W. B. *Polym. Bull.* **2008**, *59*, 749.
26. Lecamp, L.; Pavillon, C.; Lebaudy, P.; Bunel, C. *Eur. Polym. J.* **2005**, *41*, 169.
27. Podsiadly, R.; Podemska, K.; Szymczak, A. M. *Dyes Pigments* **2011**, *91*, 422.
28. Andrzejewska, E. *Prog. Polym. Sci.* **2001**, *26*, 605.
29. Neo, W. K.; Chan-Park, M. B.; Gao, J. X.; Dong, L. *Langmuir* **2004**, *20*, 11073.
30. Tsai, M. H.; Lin, Y. K.; Chang, C. J.; Chiang, P. C.; Yeh, J. M.; Chiu, W. M.; Huang, S. L.; Ni, S. C. *Thin Solid Films* **2009**, *517*, 5333.
31. Sultana, S.; Matsui, J.; Mitani, S.; Mitsuishi, M.; Miyashita, T. *Polymer* **2009**, *50*, 3240.
32. Chang, C. J.; Wu, M. S.; Kao, P. C. *J. Polym. Sci. Part B: Polym. Phys.* **2007**, *45*, 1152.
33. Zhi, J.; He, Y.; Xiao, M.; Nie, J. *Prog. Org. Coat.* **2009**, *66*, 35.
34. Zhu, M.; Gu, A.; Liang, G.; Yuan, L. *High. Perform. Polym.* **2013**, *25*, 594.
35. Chattopadhyay, D. K.; Sreedhar, B.; Raju, K. V. S. N. *Ind. Eng. Chem. Res.* **2005**, *44*, 1772.
36. Murayama, T. Dynamic Mechanical Analysis of Polymeric Material; Elsevier: New York, **1978**; p 1.
37. Hagen, R.; Salmen, L.; Stenberg, B. *J. Polym. Sci. Part B: Polym. Phys.* **1996**, *34*, 1997.
38. Mülazim, Y.; Kahraman, M. V.; Apohan, N. K.; Kızıltaş, S.; Güngör, A. *J. Appl. Polym. Sci.* **2011**, *120*, 2298.